2005 IEEE/RSJ International Conference on Intelligent Robots and Systems

2 1/2 D Visual Servoing with Central Catadioptric Cameras

H. Hadj Abdelkader, Y. Mezouar, N. Andreff and P. Martinet
LASMEA,
24 Avenue des Landais,
63177 Aubiere, FRANCE
hadj,mezouar,andreff,martinet@lasmea.univ-bpclermont.fr

***Abstract*— In this paper, we present how the 2 1/2 D visual servoing scheme can be used with omnidirectional cameras. Motivated by the growing interest for omnidirectional sensors on robotic applications and particularly on vision-based control, we extend this framework to the entire class of central catadioptric systems. Indeed, conventional cameras suffer from restricted field of view. Central catadioptric systems have larger fields of view thus overcoming the visibility problem encountered when using conventional cameras. The 2 1/2 D visual servoing is based on the estimation of the partial camera displacement between two views, given by the current and desired images. Geometrical relationships are exploited to enable a partial Euclidean reconstruction by decoupling the interaction between translation and rotation components of a homography matrix. First we describe how to obtain a generic homagraphy matrix for central catadioptric cameras from the projection model of an entire class of camera. Then the information obtained from the homography is used to develop a 2 1/2 D visual servoing scheme.**

***Index Terms*— Visual Servoing, Catadioptric cameras, Homography.**

I. INTRODUCTION

Vision-based servoing schemes are flexible and effective methods to control robot motions from cameras observations [15]. They are traditionally classified into three groups, namely position-based, image-based and hybrid-based control [10], [15], [19]. These three schemes make assumptions on the link between the initial, current and desired images since they require correspondences between the visual features extracted from the initial image with those obtained from the desired one. These features are then tracked during the camera (and/or the object) motion. If these steps fail the visually based robotic task can not be achieved [7]. Typical cases of failure arise when matching joint images features is impossible (for example when no joint features belongs to initial and desired images) or when some parts of the visual features get out of the field of view during the servoing. Some methods have been investigated to resolve this deficiency based on path planning [20], switching control [8], zoom adjustment [23], geometrical and topological considerations [9], [25]. However, such strategies are sometimes delicate to adapt to generic setup. Conventional cameras suffer thus from restricted field of view. There is thus significant motivation for increasing the field of view of the cameras [4]. Many applications in vision-based robotics, such as mobile robot localization [5] and navigation [28], can benefit from panoramic field of view provided by omnidirectional cameras. In the literature, there have been several methods proposed for increasing the field of view of cameras systems [4]. One effective way is to combine mirrors with conventional imaging system. The obtained sensors are referred as catadioptric imaging systems. The resulting imaging systems have been termed central catadioptric when a single projection center describes the world-image mapping. From a theoretical and practical view point, a single center of projection is a desirable property for an imaging system [1]. Baker and Nayar in [1] derive the entire class of catadioptric systems with a single viewpoint. Clearly, visual servoing applications can also benefit from such sensors since they naturally overcome the visibility constraint. Vision-based control of robotic arms, single mobile robot or formation of mobile robots appear thus in the literature with omnidirectional cameras (refer for example to [3], [6], [22], [27], [21]). Image-based visual servoing with central catadioptric cameras using points has been studied by in [3]. The use of straight lines has also been investigated in [21].

This paper is concerned with homography-based visual servo control techniques with central catadioptric cameras. This framework (called 2 1/2 D visual servoing) has been first proposed by Malis and Chaumette in [16], [19], [17]. The 2 1/2 D visual servoing scheme exploits a combination of reconstructed Euclidean information and image-space information in the control design. The 3D informations are extracted from an homography matrix relating two views of a reference plane. As a consequence, the 2 1/2 D visual servoing scheme does not require any 3D model of the target. The resulting interaction matrix is triangular with interesting decoupling properties and it has no singularity in the whole task space. Unfortunately, in such approach the image of the target is not guaranteed to remain in the camera field of view. Motivated by the desire to overcome this deficiency, we extend in this paper homography-based visual servo control techniques to an entire class of omnidirectional cameras. We describe how to obtain a generic homagraphy matrix related to a reference plane for central catadioptric cameras from a generic projection model. Then the 3D informations obtained from the homography is used to develop a 2 1/2 D visual servoing scheme.

The remainder of this paper is organized as follows. In Section II, the model of the central catadioptric image formation is presented. In Section III, we describe how the homography related to a reference plane can be obtained and exploited to estimate the partial motion of the camera. Section IV is devoted to the 2 1/2 D visual servoing control scheme. Simulated results are presented in Section V.

II. Central catadioptric imaging model

A vision system has a single viewpoint if all rays joining a world point and its projection in the image plane pass through a single point called principal projection center. Conventional perspective camera is a typical example of single viewpoint vision sensor. The well known pin-hole model assumes that the mapping of world points into points in the image plane is linear in homogeneous coordinates. There are single viewpoint systems whose geometry can not be modeled using the conventional pin-hole model. Baker and Nayar in [1] derive the entire class of catadioptric systems with a single viewpoint. They show that a central catadioptric system with a wide field of view can be built by combining an hyperbolic, elliptical or planar mirror with a perspective camera and a parabolic mirror with an orthographic camera. However the mapping between world points and points in the image plane is no longer linear. In [13], Geyer and Daniilidis introduce an unifying model for all central catadioptric imaging system where conventional perspective camera appears as a particular case.

Let $\mathcal{F}_c$ and $\mathcal{F}_m$ be the frames attached to the conventional camera and to the mirror respectively. In the sequel, we suppose that $\mathcal{F}_c$ and $\mathcal{F}_m$ are related by a translation along the Z-axis ($\mathcal{F}_c$ and $\mathcal{F}_m$ have the same orientation, refer to Figure 1). The origins C and M of $\mathcal{F}_c$ and $\mathcal{F}_m$ will be termed optical center and principal projection center respectively. The optical center C has coordinates $[0\ 0\ -\xi]^T$ with respect to $\mathcal{F}_m$ and the image plane $Z = \psi - 2\xi$ is orthogonal to the Z-axis. ξ and ψ describe the type of sensor and the shape of the mirror. They are function of mirror parameters d and p (see Tab.I and refer to [2]). Consider the unitary sphere centered in M as shown in Fig.1 and let $\mathcal{X}$ be a 3D point with coordinates $\mathbf{X} = [X\ Y\ Z]^T$ with respect to $\mathcal{F}_m$. The world point $\mathcal{X}$ is projected in the image plane into the point of homogeneous coordinates $\mathbf{x_i} = [x_i\ y_i\ 1]^T$. The image formation process can be split in three steps as:

Step 1: The 3D world point $\mathcal{X}$ is first projected on the unit sphere surface into a point of coordinates in $\mathcal{F}_m$:

$$\mathbf{X_m} = \frac{1}{\rho}\begin{bmatrix} \mathrm{X} \\ \mathrm{Y} \\ \mathrm{Z} \end{bmatrix}$$

where $\rho = \|\mathbf{X}\| = \sqrt{X^2+Y^2+Z^2}$. The projective ray $\mathbf{X_m}$ pass through the principal projection center M and the world point $\mathcal{X}$.

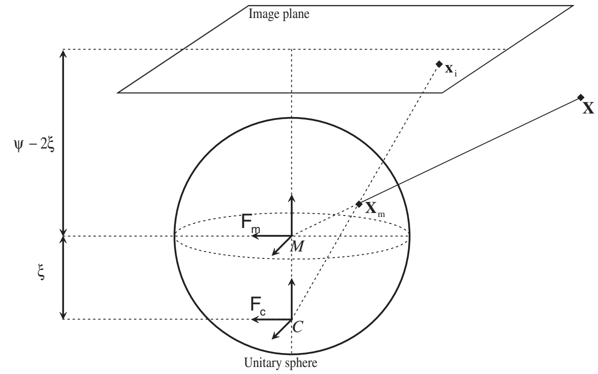

Fig. 1. Central catadioptric image formation

camera	Mirror surface	ξ	ψ
Parabolic	$z = \frac{x^2+y^2}{2a_p} - \frac{a_p}{2}$	1	$1+2p$
Hyperbolic	$\frac{(z+\frac{d}{2})^2}{a_h^2} - \frac{x^2+y^2}{b_h^2} = 1$	$\frac{d}{\sqrt{d^2+4p^2}}$	$\frac{d+2p}{\sqrt{d^2+4p^2}}$
Elliptical	$\frac{(z+\frac{d}{2})^2}{a_e^2} + \frac{x^2+y^2}{b_e^2} = 1$	$\frac{d}{\sqrt{d^2+4p^2}}$	$\frac{d-2p}{\sqrt{d^2+4p^2}}$
Planar	$z = \frac{d}{2}$	0	1
conventional	none	0	1

TABLE I

Central catadioptric cameras description: a_p, a_h, b_h, a_e, b_e depend only of the mirror intrinsic parameters d and p

Step 2: The point $\mathbf{X_m}$ lying on the unitary sphere is then perspectively projected on the plane $Z = 1 - \xi$ into a point of homogeneous coordinates $\underline{\mathbf{x}} = [\mathbf{x}^T 1]^T = \mathbf{f}(\mathbf{X})$ (where $\mathbf{x} = [x\, y]^T$) from the optical center C:

$$\underline{\mathbf{x}} = \mathbf{f}(\mathbf{X}) = \begin{bmatrix} \dfrac{X}{Z+\xi\rho} \\ \dfrac{Y}{Z+\xi\rho} \\ 1 \end{bmatrix} \tag{1}$$

Step 3: Finally the points of homogeneous coordinates $\mathbf{x_i}$ in the image plane are obtained after a plane-to-plane collineation $\mathbf{K}$ of the 2D projective point $\mathbf{x}$:

$$\mathbf{x_i} = \mathbf{K}\underline{\mathbf{x}}$$

The matrix $\mathbf{K}$ can be written as $\mathbf{K} = \mathbf{K_c}\mathbf{M}$ where the upper triangular matrix $\mathbf{K}_c$ contains the camera intrinsic parameters, and the diagonal matrix $\mathbf{M}$ the mirror intrinsic parameters:

$$\mathbf{M} = \begin{bmatrix} \psi-\xi & 0 & 0 \\ 0 & \psi-\xi & 0 \\ 0 & 0 & 1 \end{bmatrix}$$

Note that, setting $\xi = 0$, the general projection model becomes the well known perspective projection model. In the sequel, the camera and mirror intrinsic parameters are supposed known (*i.e* the collineation matrix $\mathbf{K}$ is known).

To estimate these parameters one of the algorithms proposed in [12], [2], or in [29] can be used.

Let us denote $\phi_x = \rho/|Z| = \sqrt{1 + X^2/Z^2 + Y^2/Z^2}$, the coordinates of the image point can be rewritten as:

$$x = \frac{X/Z}{1+\xi\phi_x}$$
$$y = \frac{Y/Z}{1+\xi\phi_x}$$

By combining the two previous equation, it is easy to show that ϕ_x is the solution of the following second order equation:

$$-\phi_x^2 + (x^2+y^2)(1+\xi\phi_x)^2 + 1 = 0$$

with the following solutions:

$$\phi_x = \frac{\pm\gamma_x + \xi(x^2+y^2)}{1-\xi^2(x^2+y^2)} \tag{2}$$

where $\gamma_x = \sqrt{1 + (1-\xi^2)(x^2+y^2)}$. Equation (2) shows that ϕ_x can be computed as a function of image coordinates $\mathbf{x}$ and sensor parameter ξ. Note that, ϕ_x can be computed without ambiguity since it is a positive scalar. Noticing that:

$$\mathbf{X_m} = (\phi_x^{-1} + \xi)\overline{\mathbf{x}} \tag{3}$$

where $\overline{\mathbf{x}} = [\mathbf{x}^T \ \frac{\phi_x^2}{1+\xi\phi_x}]^T$, we deduce that $\mathbf{X_m}$ can also be computed as a function of image coordinates $\mathbf{x}$ and sensor parameter ξ. The 2 1/2 D visual servoing is based on the estimation of the partial camera displacement between two views, given by the current and desired images. Geometrical relationships are exploited to compute a partial Euclidean reconstruction from a homography matrix. In the sequel, we show how the homography related to a reference plane can be obtained.

III. Scaled Euclidean reconstruction using catadioptric images

The Euclidean reconstruction from two views (structure from motion problem) plays a central role in the 2 1/2 D visual servoing scheme. Several methods were proposed to solve this problem [11]. They are generally based on the estimation of the Essential matrix. However, for control purposes, the methods based on the Essential matrix are not well suited since degenerate configurations (such as pure rotational motion) can induce unstable behavior of the control scheme. The structure from motion problem can also be solved using an homography matrix related to a virtual plane. Homography matrix and Essential matrix based approaches do not share the same degenerate configurations, for example pure rotational motion is not a degenerate configuration when using homography-based method. To design a control scheme based on partial Euclidean reconstruction, it is thus preferable to use Homography-based approaches. The epipolar geometry of central catadioptric system has been more recently investigated [14], [26]. The central catadioptric fundamental and essential matrices share similar degenerate configurations that those observed with conventional perspective cameras. In the sequel, assuming that the sensor is calibrated, we derive from the generic projection model geometrical homographic relationships between two omnidirectional views of a virtual plane.

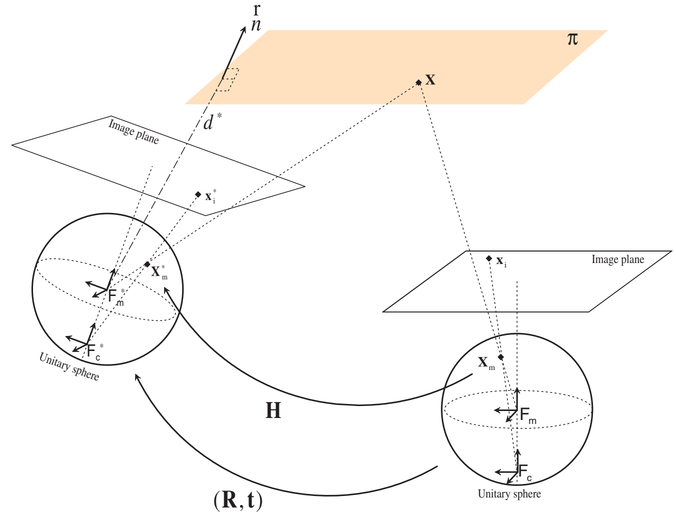

Fig. 2. Motion and structure parameters

Consider the camera motion defined by a rotation matrix $\mathbf{R}$, and a translation vector $\mathbf{t}$ between the mirror frames $\mathcal{F}_m$ and $\mathcal{F}_m^*$ (see Figure 2). Consider a 3-D reference plane (π) given in $\mathcal{F}_m^*$ by the vector $\pi^{*T} = [\mathbf{n}^* \ -d^*]$, where $\mathbf{n}^*$ is its unitary normal in $\mathcal{F}_m^*$ and d^* is the distance from (π) to the origin of $\mathcal{F}_m^*$. Let $\mathcal{X}$ be a 3-D point with coordinates $\mathbf{X} = [X \ Y \ Z]^T$ with respect to $\mathcal{F}_m$ and with coordinates $\mathbf{X} = [X^* \ Y^* \ Z^*]^T$ with respect to $\mathcal{F}_m^*$. Its projection in the unit sphere for the two camera positions are:

$$\begin{aligned}\mathbf{X_m} &= (\phi_x^{-1}+\xi)\overline{\mathbf{x}} = \tfrac{1}{\rho}\begin{bmatrix} X & Y & Z\end{bmatrix}^T \\ \mathbf{X_m^*} &= (\phi_{x^*}^{-1}+\xi)\overline{\mathbf{x}}^* = \tfrac{1}{\rho^*}\begin{bmatrix} X^* & Y^* & Z^*\end{bmatrix}^T\end{aligned} \tag{4}$$

Using the homogenous coordinates $\underline{\mathbf{X}} = [X \ Y \ Z \ H]^T$ and $\underline{\mathbf{X}}^* = [X^* \ Y^* \ Z^* \ H^*]^T$, we can write:

$$\rho(\phi_x^{-1}+\xi)\overline{\mathbf{x}} = \begin{bmatrix}\mathbf{I_3} & 0\end{bmatrix}\underline{\mathbf{X}} = \begin{bmatrix}\mathbf{R} & \mathbf{t}\end{bmatrix}\underline{\mathbf{X}}^* \tag{5}$$

The distance $d(\mathcal{X},\pi)$ from the world point $\mathcal{X}$ to the plane (π) is given by the scalar product $\pi^{*T}\cdot\underline{\mathbf{X}}^*$ and:

$$d(\mathcal{X},\pi) = \rho^*(\phi_{x^*}^{-1}+\xi)\mathbf{n}^{*T}\overline{\mathbf{x}}^* - d^*H^*$$

As a consequence, the unknown homogenous component H^* is given by:

$$H^* = \frac{\rho^*(\phi_{x^*}^{-1}+\xi)}{d^*}\mathbf{n}^{*T}\overline{\mathbf{x}}^* - \frac{d(\mathcal{X},\pi)}{d^*} \tag{6}$$

The homogeneous coordinates of $\mathcal{X}$ with respect to $\mathcal{F}_m^*$ can be rewritten as:

$$\underline{\mathbf{X}}^* = \rho^*(\phi_{x^*}^{-1} + \xi) \begin{bmatrix} \mathbf{I_3} & 0 \end{bmatrix}^T \overline{\mathbf{x}}^* + \begin{bmatrix} \mathbf{0_{1\times 3}} & H^* \end{bmatrix}^T \quad (7)$$

By combining the Equations (6) and (7), we obtain:

$$\underline{\mathbf{X}}^* = \rho^*(\phi_{x^*}^{-1} + \xi)\mathbf{A}_\pi^* \overline{\mathbf{x}}^* + \mathbf{b}_\pi^* \quad (8)$$

where

$$\mathbf{A}_\pi^* = \begin{bmatrix} \mathbf{I_3} & \frac{\mathbf{n}^*}{d^*} \end{bmatrix}^T \quad \text{and} \quad \mathbf{b}_\pi^* = \begin{bmatrix} \mathbf{0_{1\times 3}} & -\frac{d(\mathcal{X},\pi)}{d^*} \end{bmatrix}$$

According to (8), the expression (5) can be rewritten as:

$$\rho(\phi_x^{-1} + \xi)\overline{\mathbf{x}} = \rho^*(\phi_{x^*}^{-1} + \xi)\mathbf{H}_\pi \overline{\mathbf{x}}^* + \alpha \mathbf{t} \quad (9)$$

with $\mathbf{H}_\pi = \mathbf{R} + \frac{\mathbf{t}}{d^*}\mathbf{n}^{*T}$ and $\alpha = -\frac{d(\mathcal{X},\pi)}{d^*}$.

$\mathbf{H}_\pi$ is the Euclidean homography matrix written as a function of the camera displacement and of the plane coordinates with respect to $\mathcal{F}_m^*$. It has the same form as in the conventional perspective case (it is decomposed into a rotation matrix and a rank 1 matrix). If the world point $\mathcal{X}$ belongs to the reference plane (π) (*i.e* $\alpha = 0$) then Equation (9) becomes:

$$\overline{\mathbf{x}} = \beta_{x,x^*}\mathbf{H}_\pi \overline{\mathbf{x}}^* \quad (10)$$

where $\beta_{x,x^*} = \frac{\phi_{x^*}^{-1}+\xi}{\phi_x^{-1}+\xi}$. Note that the Equation (10) can be turned into a linear homogeneous equation $\overline{\mathbf{x}} \otimes \mathbf{H}_\pi \overline{\mathbf{x}}^* = \mathbf{0}$ (where $\otimes$ denotes the cross-product). As usual, the homography matrix related to (π), can thus be estimated up to a scale factor, using four couples of coordinates $(\mathbf{x}_k; \mathbf{x}_k^*)$, $k = 1 \cdots 4$, corresponding to the projection in the image space of world points $\mathcal{X}_k$ belonging to (π). If only three points belonging to (π) are available then at least five supplementary points are necessary to estimate the homography matrix by using for example the linear algorithm proposed in [17]. From the estimated homography matrix, the camera motion parameters (that is the rotation $\mathbf{R}$ and the scaled translation $\mathbf{t}_{d^*} = \frac{\mathbf{t}}{d^*}$) and the structure of the observed scene (for example the vector $\mathbf{n}^*$) can thus be determined (refer to [11], [30]). It can also be shown that the ratio $\sigma = \frac{\rho}{\rho^*}$ can be estimated as follow:

$$\sigma = \frac{\rho}{\rho^*} = (1 + \mathbf{n}^{*T}\mathbf{R}^T \mathbf{t}_{d^*})\frac{(\phi_{x^*}^{-1} + \xi)n^{*T}\overline{\mathbf{x}}^*}{(\phi_x^{-1} + \xi)n^{*T}\mathbf{R}^T\overline{\mathbf{x}}} \quad (11)$$

This parameter is used in our 2 1/2 D visual servoing control scheme.

IV. 2 1/2 D Visual Servoing with Central Catadioptric Cameras

As usual when designing a 2 1/2 D visual servoing, the feature vector used as input of the control law combines 2-D and 3-D informations [19]:

$$\mathbf{s} = [\mathbf{s}_i^T \ \theta \mathbf{u}^T]^T \quad \text{and} \quad \mathbf{s}_i = [x \, y \, \varrho]^T$$

where x and y are the current coordinates of a chosen catadioptric image point given by Equation (1), $\varrho = \log(\rho)$ and, $\mathbf{u}$ and θ are respectively the axis and the rotation angle obtained from $\mathbf{R}$ (rotation matrix between the mirror frame when the camera is in these current and desired positions). The task function $\mathbf{e}$ to regulate to 0 [24] is given by:

$$\mathbf{e} = \mathbf{s} - \mathbf{s}^* = [x - x^*,\, y - y^*,\, \Gamma,\, \theta \mathbf{u}^T]^T \quad (12)$$

where $\mathbf{s}^*$ is the desired value of $\mathbf{s}$ and $\Gamma = \log\left(\frac{\rho}{\rho^*}\right) = \log(\sigma)$. The first two components of $\mathbf{s}_i - \mathbf{s}_i^*$ are computed from the normalized current and desired catadioptric images, and its last components can be estimated using Equation (11). The rotational part of $\mathbf{e}$ is estimated using partial Euclidean reconstruction from the homography matrix derived in Section III. The exponential decay of $\mathbf{e}$ toward $\mathbf{0}$ can be obtained by imposing $\dot{\mathbf{e}} = -\lambda \mathbf{e}$ (λ being a proportional gain), the corresponding control law is:

$$\tau = -\lambda \mathbf{L}^{-1}(\mathbf{s} - \mathbf{s}^*) \quad (13)$$

where τ is a 6-dimensional vector denoting the velocity screw of the central catadioptric camera. It contains the instantaneous angular velocity ω and the instantaneous linear velocity v. $\mathbf{L}$ is the interaction matrix related to $\mathbf{s}$. It links the variation of $\mathbf{s}$ to the camera velocity: $\dot{\mathbf{s}} = \mathbf{L}\tau$. It is thus necessary to compute the interaction matrix in order to derive the control law given by the Equation (13). The time derivative of the rotation vector $\mathbf{u}\theta$ can be expressed as a function of the catadioptric camera velocity vector τ as:

$$\frac{d(\mathbf{u}\theta)}{dt} = [\mathbf{0_3} \quad \mathbf{L}_\omega]\,\tau \quad (14)$$

where $\mathbf{L}_\omega$ is given by [19]:

$$\mathbf{L}_\omega(\mathbf{u}, \theta) = \mathbf{I_3} - \frac{\theta}{2}[\mathbf{u}]_\times + \left(1 - \frac{\operatorname{sinc}(\theta)}{\operatorname{sinc}^2(\frac{\theta}{2})}\right)[\mathbf{u}]_\times^2 \quad (15)$$

with $\operatorname{sinc}(\theta) = \frac{\sin(\theta)}{\theta}$ and $[\mathbf{u}]_\times$ being the antisymmetric matrix associated to vector $\mathbf{u}$.

To control the 3 translational degrees of freedom (*ddl*), the visual observations and the ratio σ expressed in (11) are used. Consider a 3-D point $\mathcal{X}$, lying on the the reference plane (π), as the reference point. The time derivative of its coordinates, with respect to the current catadioptric frame $\mathcal{F}_m$, is given by:

$$\dot{\mathbf{X}} = [-\mathbf{I_3} \ \ [\mathbf{X}]_\times]\,\tau \quad (16)$$

$[\mathbf{X}]_\times$ being the antisymmetric matrix associated to the vector $\mathbf{X}$. The time derivative of $\mathbf{s}_i$ can be written as:

$$\dot{\mathbf{s}}_i = \frac{\partial \mathbf{s}_i}{\partial \mathbf{X}}\dot{\mathbf{X}} \quad (17)$$

with:

$$\frac{\partial \mathbf{s}_i}{\partial \mathbf{X}} = \frac{1}{\rho(Z + \xi\rho)^2}\begin{bmatrix} \rho Z + \xi(Y^2 + Z^2) & -\xi XY & -X(\rho + \xi Z) \\ -\xi XY & \rho Z + \xi(X^2 + Z^2) & -Y(\rho + \xi Z) \\ \frac{X(Z+\xi\rho)^2}{\rho} & \frac{Y(Z+\xi\rho)^2}{\rho} & \frac{Z(Z+\xi\rho)^2}{\rho} \end{bmatrix}$$

By combining the equations (16), (17) and (11), it can be shown that:

$$\dot{\mathbf{s}}_i = [\mathbf{A}\ \ \mathbf{B}]\,\tau \tag{18}$$

with

$$\mathbf{A} = \frac{1}{\sigma\rho^*}\begin{bmatrix} -\frac{1+x^2(1-\xi(\gamma_x+\xi))+y^2}{\gamma_x+\xi} & \xi xy & x\gamma_x \\ \xi xy & -\frac{1+x^2+y^2(1-\xi(\gamma_x+\xi))}{\gamma_x+\xi} & y\gamma_x \\ \eta_x x & \eta_x y & (\eta_x-1)\xi \end{bmatrix}$$

and

$$\mathbf{B} = \begin{bmatrix} xy & -\frac{(1+x^2)\gamma_x-\xi y^2}{\gamma_x+\xi} & y \\ \frac{(1+y^2)\gamma_x-\xi x^2}{\gamma_x+\xi} & -xy & -x \\ 0 & 0 & 0 \end{bmatrix}$$

where:

$$\gamma_x = \sqrt{1+(1-\xi^2)(x^2+y^2)}$$

$$\eta_x = \frac{\xi^2+\sqrt{(x^2+y^2)(1-\xi^2)+\xi^2}}{x^2+y^2+\xi^2}$$

The task function $\mathbf{e}$ (see Equation (12)) can thus be regulated to $\mathbf{0}$ using the control law (Equation (13)) with the following interaction matrix $\mathbf{L}$:

$$\mathbf{L} = \begin{bmatrix} \mathbf{A} & \mathbf{B} \\ \mathbf{0_3} & \mathbf{L}_\omega \end{bmatrix} \tag{19}$$

In practice, an approximated interaction matrix $\widehat{\mathbf{L}}$ is used. The parameter ρ^* can be estimated only once during a off-line learning stage.

V. Simulation results

In this section, we present simulation results of 2 1/2 D visual servoing with a catadioptric camera in eye-in-hand configuration. The catadioptric camera used is an hyperbolic mirror combined with a perspective camera (similar results are obtained with a catadioptric camera combining a parabolic mirror and an orthographic lens, these results are not presented in this paper). From an initial position the catadioptric camera mounted on the robot has to reach a desired position known as a desired 2 1/2 D observation vector $\mathbf{s}^*$. Image noise has been added (additive noise with maximum amplitude of 2 pixels) to the coordinates of image points. The normalized coordinates and the interaction matrix are computed using erroneous internal camera parameters.

The initial and desired attitudes of the catadioptric camera are plotted in the Figure 3. This figure also shows the 3-D camera trajectory from its initial position to the desired one. Figure 4(a) shows the initial (blue *) and desired (red *) images of the observed target. It shows also the trajectory of the point (green trace) in the image plane (the controlled image point has a black trace trajectory). The norm of the error vector is given in Figure 4(b). As can been seen in the Figures 5(a) and 5(b) showing the errors between desired and current observation vectors the task is correctly realized. The translational and rotational camera velocities are given in Figures 6(a) and 6(b) respectively.

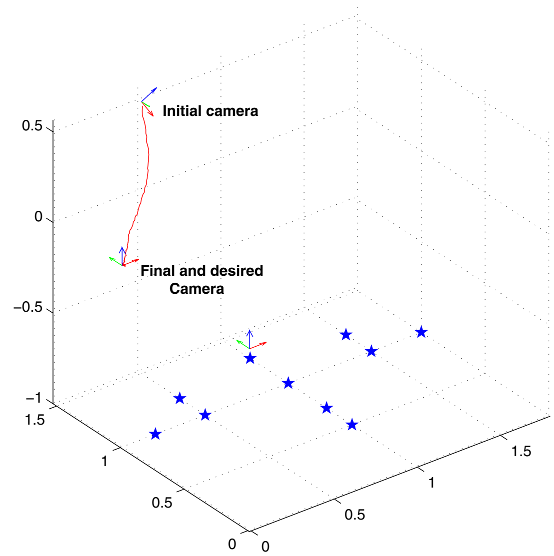

Fig. 3. 3-D Trajectories of the catadioptric camera [meters]

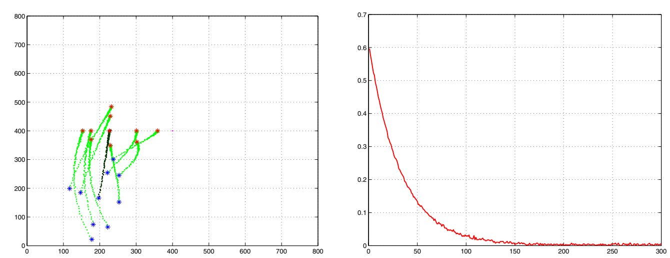

(a) (b)

Fig. 4. (a) Trajectories in the image of the target points [pixels]. (b) norm of the error vector

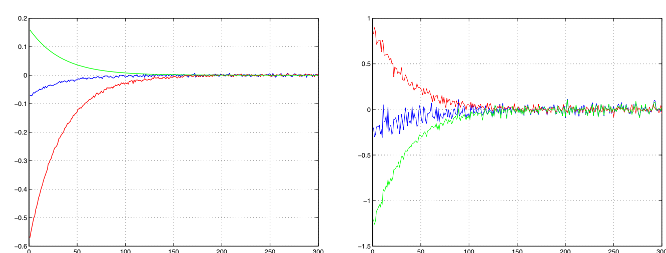

(a) (b)

Fig. 5. (a) Error vector: $(\mathbf{s}_i - \mathbf{s}_i^*)$ [meters], (b) rotation vector: $\mathbf{u}\theta$ [rad]

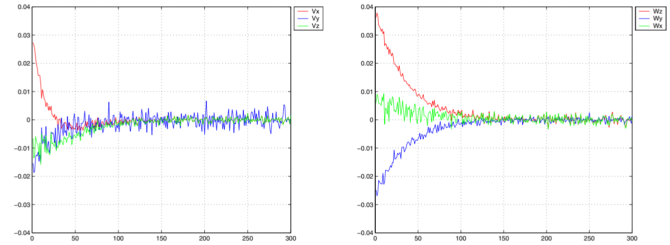

(a) (b)

Fig. 6. (a) Translational velocity [m/s]. (b) rotational velocity [rad/s]

VI. Conclusion

In this paper, we have described how the 2 1/2 D visual servoing scheme can be used with omnidirectional cameras. Geometrical relationships have been derived from the projection model of an entire class of camera (including conventional perspective cameras). These relationships have been exploited to obtain a homographic mapping between two views of a reference plane which allows to estimate structure and motion parameters. These parameters were then used to develop a 2 1/2 D visual servoing scheme.

The robustness of 2 1/2 D visual servoing with respect to calibration errors has been analyzed in [19] in the case of conventional perspective camera. In the case of omnidirectional cameras, this study is an important theoretical point that has to be addressed.

References

[1] S. Baker and S. K. Nayar. A theory of single-viewpoint catadioptric image formation. *International Journal of Computer Vision*, 35(2):1–22, November 1999.

[2] J. Barreto and H. Araujo. Geometric properties of central catadioptric line images. In *7th European Conference on Computer Vision, ECCV'02*, pages 237–251, Copenhagen, Denmark, May 2002.

[3] J. P. Barreto, F. Martin, and R. Horaud. Visual servoing/tracking using central catadioptric images. In *ISER2002 - 8th International Symposium on Experimental Robotics*, pages 863–869, Bombay, India, July 2002.

[4] R. Benosman and S. Kang. *Panoramic Vision*. Springer Verlag ISBN 0-387-95111-3, 2000.

[5] P. Blaer and P.K. Allen. Topological mobile robot localization using fast vision techniques. In *IEEE International Conference on Robotics and Automation*, pages 1031–1036, Washington, USA, May 2002.

[6] D. Burshka, J. Geiman, and G. Hager. Optimal landmark configuration for vision based control of mobile robot. In *IEEE International Conference on Robotics and Automation*, pages 3917–3922, Tapei, Taiwan, September 2003.

[7] F. Chaumette. Potential problems of stability and convergence in image-based and position-based visual servoing. *The Confluence of Vision and Control, D. Kriegman, G. Hager, A. Morse (eds), LNCIS Series, Springer Verlag*, 237:66–78, 1998.

[8] G. Chesi, K. Hashimoto, D. Prattichizzo, and A. Vicino. A switching control law for keeping features in the field of view in eye-in-hand visual servoing. In *IEEE International Conference on Robotics and Automation*, pages 3929–3934, Taipei, Taiwan, September 2003.

[9] Noah J. Cowan, Joel D. Weingarten, and Daniel E. Koditschek. Visual servoing via navigation functions. *IEEE Transactions on Robotics and Automation*, 18(4):521–533, August 2002.

[10] B. Espiau, F. Chaumette, and P. Rives. A new approach to visual servoing in robotics. *IEEE Transactions on Robotics and Automation*, 8(3):313–326, June 1992.

[11] O. Faugeras and F. Lustman. Motion and structure from motion in a piecewise planar environment. *Int. Journal of Pattern Recognition and Artificial Intelligence*, 2(3):485–508, 1988.

[12] C. Geyer and K. Daniilidis. Catadioptric camera calibration. In *Proceedings 7th International Conference on Computer Vision, ICCV99*, pages 398–403, Corfu, Greece, 1999.

[13] C. Geyer and K. Daniilidis. A unifying theory for central panoramic systems and practical implications. In *European Conference on Computer Vision*, volume 29, pages 159–179, Dublin, Ireland, May 2000.

[14] C. Geyer and K. Daniilidis. Mirrors in motion: Epipolar geometry and motion estimation. In *International Conference on Computer Vision, ICCV03*, pages 766–773, Nice, France, 2003.

[15] S. Hutchinson, G.D. Hager, and P.I. Corke. A tutorial on visual servo control. *IEEE Transactions on Robotics and Automation*, 12(5):651–670, October 1996.

[16] E. Malis. *Contributions la modlisation et la commande en asservissement visuel*. PhD thesis, Universit de Rennes I, IRISA, November 1998.

[17] E. Malis and F. Chaumette. 2 1/2 d visual servoing with respect to unknown objects through a new estimation scheme of camera displacement. *International Journal of Computer Vision*, 37(1):79–97, June 2000.

[18] E. Malis, F. Chaumette, and S. Boudet. *2D1/2 Visual Servoing*. Publication interne 1166, IRISA Rennes, France, 1998.

[19] E. Malis, F. Chaumette, and S. Boudet. 2 1/2 d visual servoing. *IEEE Transactions on Robotics and Automation*, 15(2):238–250, April 1999.

[20] Y. Mezouar and F. Chaumette. Path planning for robust image-based control. *IEEE Transactions on Robotics and Automation*, 18(4):534–549, August 2002.

[21] Y. Mezouar, H. Haj Abdelkader, P. Martinet, and F. Chaumette. Central catadioptric visual servoing from 3d straight lines. In *IEEE/RSJ Int. Conf. on Intelligent Robots and Systems, IROS'04*, volume 1, pages 343–349, Sendai, Japan, September 2004.

[22] A. Paulino and H. Araujo. Multiple robots in geometric formation: Control structure and sensing. In *International Symposium on Intelligent Robotic Systems*, pages 103–112, University of Reading, UK, July 2000.

[23] E. Malis S. Benhimane. Vision-based control with respect to planar and non-planar objects using a zooming camera. In *IEEE International Conference on Advanced Robotics*, pages 863–869, July 2003.

[24] C. Samson, B. Espiau, and M. Le Borgne. *Robot Control : The Task Function Approach*. Oxford University Press, 1991.

[25] B. Thuilot, C. Cariou, P. Martinet, and M. Berducat. Automatic guidance of a farm tractor relying on a single cp-dgps. *Autonomous Robots*, 13, 2002.

[26] Tomas Pajdla Tomas Svoboda and Vaclav Hlavac. Motion estimation using central panoramic cameras. In *IEEE Conference on Intelligent Vehicles*, Stuttgart, Germany, October 1998.

[27] R. Vidal, O. Shakernia, and S. Sastry. Formation control of nonholonomic mobile robots with omnidirectional visual servoing and motion segmentation. In *IEEE International Conference on Robotics and Automation*, pages 584–589, Taipei, Taiwan, September 2003.

[28] N. Winter, J. Gaspar, G. Lacey, and J. Santos-Victor. Omnidirectional vision for robot navigation. In *Proc. IEEE Workshop on Omnidirectional Vision, OMNIVIS*, pages 21–28, South Carolina, USA, June 2000.

[29] Xianghua Ying and Zhanyi Hu. Catadioptric camera calibration using geometric invariants. *IEEE Transactions on Pattern Analysis and Machine Intelligence*, 26(10):1260–1271, October 2004.

[30] Z. Zhang and A. R. Hanson. Scaled euclidean 3d reconstruction based on externally uncalibrated cameras. In *IEEE Symposium on Computer Vision*, Coral Gables, FL, 1995.